Dynamics and Control of a VTOL quad-thrust aerial robot

Joshua N Portlock and Samuel N Cubero

Mechanical & Mechatronic Engineering, Curtin University of Technology, Perth

1 Introduction

Some possible useful applications for Vertical Take-Off & Landing (VTOL) Unmanned Aerial Vehicles (UAVs) include remote video surveillance by security personnel, scouting missions or munitions delivery for the military, filming sports events or movies from almost any angle and transporting or controlling equipment. This paper describes the design, control and performance of a low-cost VTOL quadrotor UAV, known as the QTAR (Quad Thrust Aerial Robot).

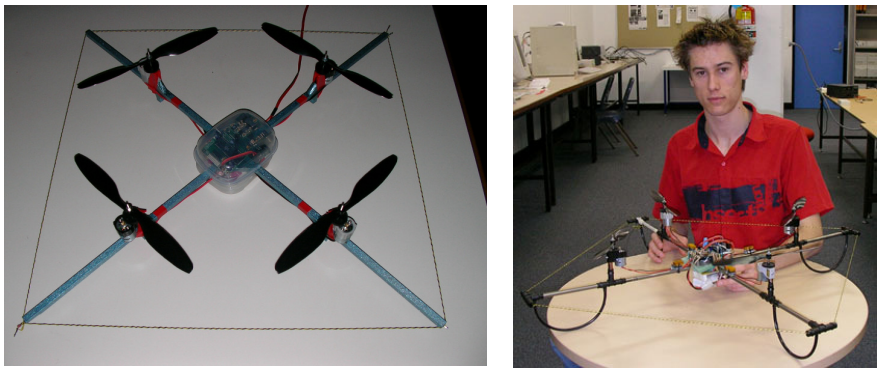

Fig. 1. QTAR Prototypes built at Curtin University of Technology

The QTAR is capable of stationary hover and omnidirectional flight; whereby pitch angle, roll angle, yaw rate and thrust can be controlled independently, while translation is subsequently controlled by these primary four inputs (tilting the thrust vector in the desired direction). The QTAR project had succeeded in developing and implementing a novel "attitude estimator" controller using very low cost components which provide sufficiently accurate tilt angles and state information for very responsive closed-loop feedback control of all flight degrees of freedom. The Attitude Control System (ACS) of the QTAR serves to automatically

control all four motor thrusts simultaneously to stabilize all the main flight degrees of freedom (translation forwards and backwards, left and right and rotating on the spot yaw) except for altitude control. Thus, the QTAR saves a remote operator a great deal of adjustment and control effort, allowing the user to focus more on navigation and performing tasks rather than on continuously adjusting several motor speeds to maintain stability and control, manually.

The quadrotor configuration employs four independent fixed-pitch rigid propellers for both propulsion and control. Each propeller is powered by its own electric motor, symmetrically positioned on each end of a "+" shape. The photos in Fig. 1 show two prototypes of the QTAR UAV that were designed, built, programmed and successfully flown at Curtin University of Technology, Western Australia, in 2005. A demonstration video can be viewed online [10].

2 Current "state of the art" in quadrotor UAVs

Triple and quadrotor configurations are the only types of VTOL UAV that employ rotor speed for control. Therefore control is actuated with no extra mechanical complexity, weight penalty or energy losses, commonly associated with swash plates, control surfaces or tail rotors. A triple rotor VTOL UAV, like the Tribelle [5], is the mechanically simplest configuration, however it cannot achieve independent control over roll and yaw moves, as they are coupled.

At the time of initiating this project in 2005, the Draganflyer™ by RC Toys [5] was the only commercially available quad-rotor, selling at over $1300AUD [12]. Many other VTOL UAV researchers have used this platform for their research [1], [2], [11], [3], [7]. In early 2005, the Draganflyer only had rate-gyro feedback for damping its attitude rates and little attitude stabilization or correction capabilities, hence a human operator had to focus much attention on maintaining stability and control.

Later in 2005, RC Toys released their Ti (Thermal Intelligence) system. This performs some angular feedback to level out the Draganflyer when no user input is given; however the thermal horizon sensors are only accurate outdoors, at altitudes above the urban canopy [12]. As well as this attitude control limitation, the Draganflyer was limited to only 10 minutes of flight time, a small 1.5:1 thrust to weight ratio and a payload of less than 100 grams.

These performance limitations were the key motivators to develop a more powerful quadrotor platform with an attitude control system capable of functioning indoors. Using low-cost commercially available "off the shelf" components, the goals of the QTAR project were to achieve a 2:1 thrust/weight ratio for improved control, flight endurance greater than 15 minutes and a 200 gram payload capacity, enough to carry an onboard wireless camera and additional equipment or sensors. These capabilities would satisfy many VTOL UAV applications.

3 Design of the Propulsion System

Electrical DC motor drives were chosen in preference to Internal Combustion (IC) engines, which are quite noisy and involve high maintenance and operating costs. It was desirable to keep the maximum span of the QTAR within the width of a typical doorway to allow flight transitions into and through buildings. Therefore a propeller diameter of 10" (10 inches, or 254 mm) was selected to maintain a maximum span under 750 mm. Dual-bladed propellers (prop) were selected because they have much lower inertia and thus respond faster to thrust command signals than four-bladed props. Two different 10" diameter props, one with an 8 inch pitch and another with a 4.5" pitch were compared in tests. It was found that the 4.5" prop was more efficient, as it produced more thrust for the same amount of power. The GWS 380 brushed motor (rated at 70 Watts continuous) with a 5.33:1 gearbox was determined to be suitable for the 10" by 4.5" prop. This was compared with two different types of brushless motors (a gear-boxed in-runner and a direct-drive out-runner). The brushless motors both performed marginally better than the brushed motor, however, the brushed motors were chosen to simplify the controller and minimize costs. The thrust verses voltage (duty cycle) relationship for the brushed motor was close to linear, making simple open-loop speed control possible. The following plot in Fig. 2 illustrates the QTAR propulsion performance compared to two other commercially available quadrotor aircraft: the RC Toys Draganflyer™ and the Silverlit X-UFO™.

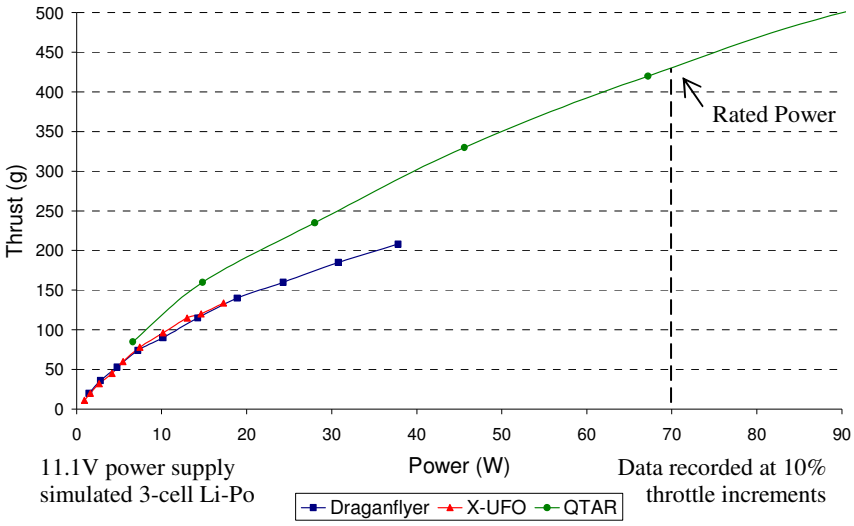

Fig. 2. Quadrotor Propulsion Performance Comparision

This data illustrates QTAR's superior efficiency, while the Draganflyer and X-UFO both had similar, lower thrust/power characteristics. This plot also illustrates

the maximum collective thrusts of 510 grams for the X-UFO and 620 grams for the Draganflyer. The QTAR system was capable of producing more than 2 kg of collective thrust. The final QTAR prototype weighs about 450 grams. The energy density of Lithium Polymer (Li-Po) batteries at the time was calculated to be 145 mWh/gram, so the maximum battery capacity while retaining a 2:1 thrust/weight ratio and carrying a 200 gram payload was 2490 mAh. This gave a theoretical endurance of 18 minutes. Even using the 2100 mAh battery we received from [13], the QTAR achieved flight times greater than 15 minutes.

4 Dynamic Modelling of Attitude

The dynamic attitude model was derived from Newton's Laws. The gyroscopic procession of each rotor cancels out due to the counter-rotating pairs, which removes any coupling between the pitch and roll dynamics. Due to the low rotor inertia relative to the craft's rotational inertia, the response of the electric motor was significantly faster than the attitude dynamics, so the motor response was assumed negligible in this model. The total collective thrust, F_T, is the sum of all four rotor forces. (subscripts are T=Total, F=Front, B=Back, L=Left, R=Right)

$$F_T = F_F + F_B + F_L + F_R \tag{1}$$

This collective thrust is nominally equal to the gravitational force when hovering, however, it can be varied by the pilot with the throttle input up to a maximum of $2\times F_g$, due to the 2:1 thrust/weight ratio. When QTAR is in a stationary hover, F_T equals the weight force of the entire aircraft due to gravity.

Yaw Dynamics

A quadrotor has two sets of counter-rotating propellers, therefore, the net yaw moment generated from aerodynamic drag is cancelled out in neutral flight. This eliminates the need for a tail rotor that normally wastes 12% of the power in a conventional helicopter [4], [9]. Furthermore, a yaw moment is induced on a quadrotor by proportionally varying the speeds of the counter-rotating pairs, as illustrated in Fig. 7. The thrust variation, V_ψ, is given by

$$V_\psi \le \frac{\tau_{\max}}{k} \quad (k = 2 \text{ or } 4 \text{ to avoid motor saturation, } \tau_{\max} = \text{max. Torque }) \tag{2}$$

From $\tau_\psi = I_z \times \ddot{\psi}$, where I_z is the mass moment of inertia, yaw acceleration is

$$\ddot{\psi} = \frac{\tau_\psi}{I_z} \quad (\text{where } \psi = \text{Yaw angle}) \tag{3}$$

Yaw moment is the sum of all rotor torques (CW=Clockwise, CCW=counter CW)

$$\tau_\psi = \sum \tau_r = \tau_{CW} - \tau_{CCW} = (\tau_L + \tau_R) - (\tau_F + \tau_B) \tag{4}$$

In Fig. 3, the magnitudes of thrust forces are set so that $F_L = F_R$ are both larger than $F_F = F_B$. The increased drag of the motors with higher thrust will create a net reaction moment that will rotate the body in one yaw direction. Similarly, the body can be rotated in the opposite yaw direction by reversing the relative magnitudes of the above pairs of thrust forces, where the thrusts of $F_F = F_B$ are greater than the thrusts of $F_L = F_R$. Note that during yaw movement of the QTAR $\tau_\psi \neq 0$ (net torque on the body), ie. the sum of reaction moments is non-zero. Note that the size of each thrust is proportional to the size of each arrow, where the largest arrow represents a high thrust, the medium sized arrow represents a medium thrust (idling thrust for zero net rise or fall for each motor) and the smallest arrow represents a weak thrust. When the QTAR body is not rising or dropping in altitude, the sum of all thrusts equals the weight force due to gravity.

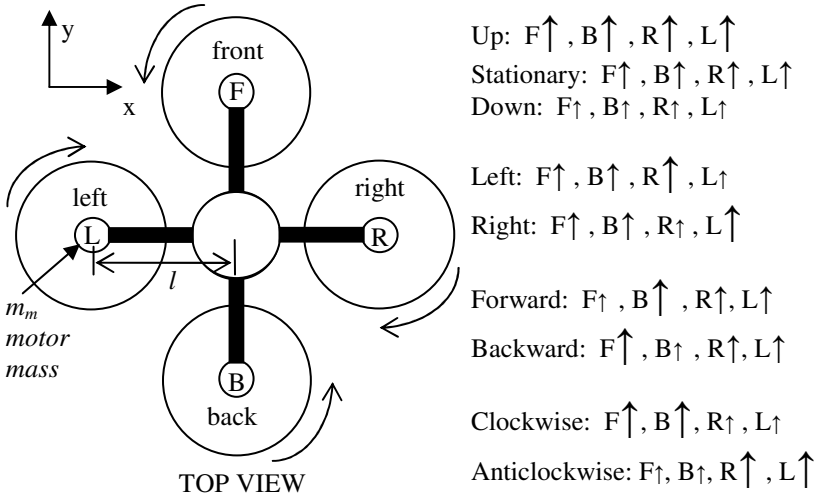

Fig. 3. Plus "+" configuration for flight control (size of arrow is proportional to thrust)

The torque on each rotor, caused by aerodynamic drag, is proportional to the thrust by a scalar constant k_τ. Therefore, Equation (4) becomes

$$\tau_\psi = (k_\tau \mathrm{V}_\psi + k_\tau \mathrm{V}_\psi) - (-k_\tau \mathrm{V}_\psi - k_\tau \mathrm{V}_\psi) = 4k_\tau \mathrm{V}_\psi \tag{5}$$

The *z*-axis "Moment Of Inertia" (MOI) of the QTAR is the sum of all point mass inertias about the z-axis (assuming battery and controller inertia is negligible due to their masses being located predominantly at the "Centre Of Gravity", or COG).

$$I_z = \sum I_m = 4m_m l^2 \quad \text{(where } m_m \text{ is a single motor \& arm mass)} \tag{6}$$

Therefore, substituting Equations (5) and (6) into (3), gives the equation of motion for yaw acceleration:

$$\ddot{\psi} = \frac{\tau_{\psi}}{I_z} = \frac{4k_{\tau}\mathrm{V}_{\psi}}{4m_m l^2} = \frac{k_{\tau}\mathrm{V}_{\psi}}{m_m l^2} \tag{7}$$

Pitch and Roll Dynamics

Due to the symmetrical nature of the quadrotor configuration, pitch and roll can be represented by the same model. Fig. 3 illustrates the thrust variations required to induce a moment about the y-axis for rolling. The yaw deviation limit is thus

$$\mathrm{V}_{\phi,\theta} \leq \frac{F_{\max}}{k} \quad (k = 2 \text{ or } 4 \text{ to avoid motor saturation, } F_{\max} = \text{maximum Force}) \tag{8}$$

The equation of motion for this pitching or rolling moment is derived from the sum of moments about the y-axis:

$$\sum \tau_{\theta} = I_y \times \ddot{\theta} \tag{9}$$

The thrust deviation for one motor can be calculated as

$$\mathrm{V}_{\theta} = (F_B - F_F)/2 \tag{10}$$

Therefore the sum of the moments is

$$\sum \tau_{\theta} = 2\mathrm{V}_{\theta} l \tag{11}$$

The *y*-axis moment of inertia of QTAR is the sum of the two point mass inertias

$$I_y = \sum I_m = 2m_m l^2 \tag{12}$$

We now substitute equations (11) and (12) into (9) to find pitch acceleration.

$$\begin{aligned} \sum \tau_{\theta} &= I_y \times \ddot{\theta} \\ 2\mathrm{V}_{\theta} l &= 2m_m l^2 \times \ddot{\theta} \\ \ddot{\theta} &= \frac{2\mathrm{V}_{\theta} l}{2m_m l^2} = \frac{\mathrm{V}_{\theta}}{m_m l} \end{aligned} \tag{13}$$

Due to symmetry of the QTAR body, this also represents pitch dynamics. The dynamic equations discussed so far have treated the QTAR as a flying "+" structure. Alternatively, Professor John Billingsley from the University of Southern Queensland proposed a different control strategy involving the aircraft controlled as a flying "X" structure, whereby pairs of motors are controlled. Figure 4 shows another method for controlling the thrusts of the QTAR. Note that motors "a" and "b" are at the "front" side, "c" and "d" are at the "back" side, "a" and "c" are on the "left" side and "b" and "d" are on the "right" side of the vehicle (imagine this as a form of "diagonal flying" for the "+" structure in Fig. 3). Either "+" or "X" configurations can be used to control the QTAR successfully. For both configurations, the dynamic equation for vertical altitude acceleration will be the same, but the equation for pitch acceleration will be slightly different due to pairs of motors being controlled for the "X" configuration control method.

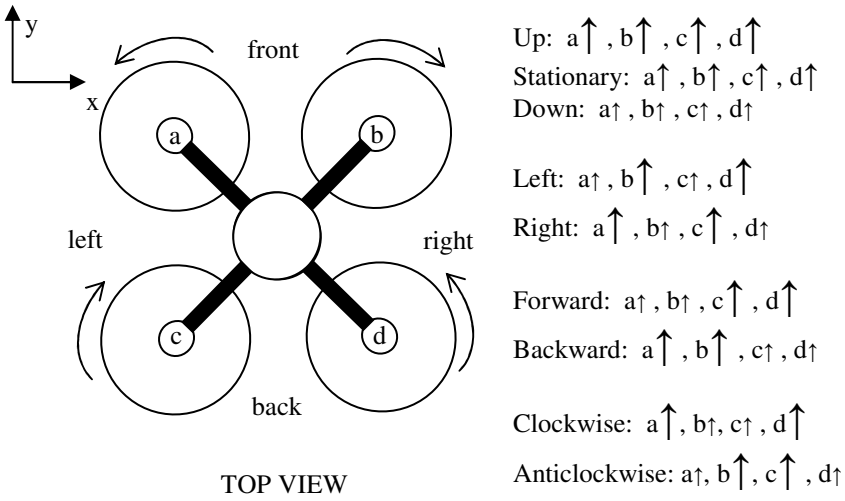

Fig. 4. "X" configuration for flight control (size of arrow is proportional to thrust)

5 Attitude Controller Design and Simulation

It is evident from the developed models that the pitch/roll dynamics are linear (if actuator saturation is avoided), time-invariant and 2nd order. Furthermore, aerodynamic drag is assumed to be negligible, therefore this system model has no natural damping, no zeros and only one pole at the origin. This means that open-loop systems will always be unstable without feedback.

With no natural damping, a proportional-only feedback controller would not adequately stabilise the attitude of the system, rather the system will require active damping. The pitch/roll controller illustrated in Fig. 5 was implemented.

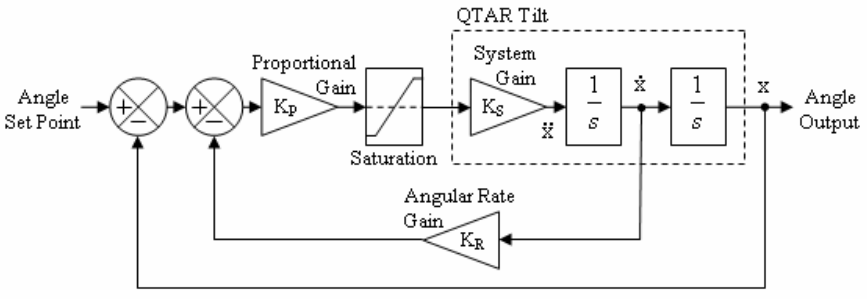

Fig. 5. Pitch/Roll Controller Block Diagram

Yaw required a different controller configuration because it was a 1st order system without a global bearing angle reference. The user input was angular-rate, which was adequate for remotely piloted control. This control method dampens the yaw rate and thus maintains a relatively constant bearing while the user yaw input is left neutral. The yaw rate controller is illustrated below in Fig. 6.

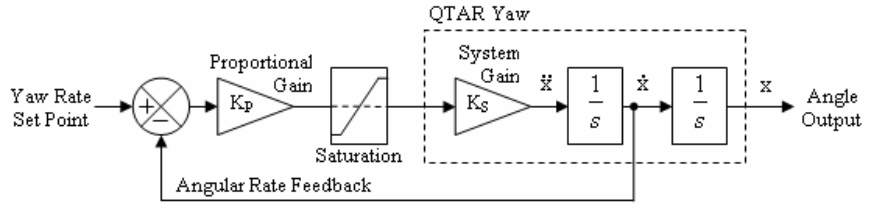

Fig. 6. Yaw Rate Controller Block Diagram

After establishing appropriate attitude controller designs, simulations were performed using MATLAB™ (by Mathworks) to evaluate the dynamic response of these controllers and sensor requirements such as states, ranges and resolutions.

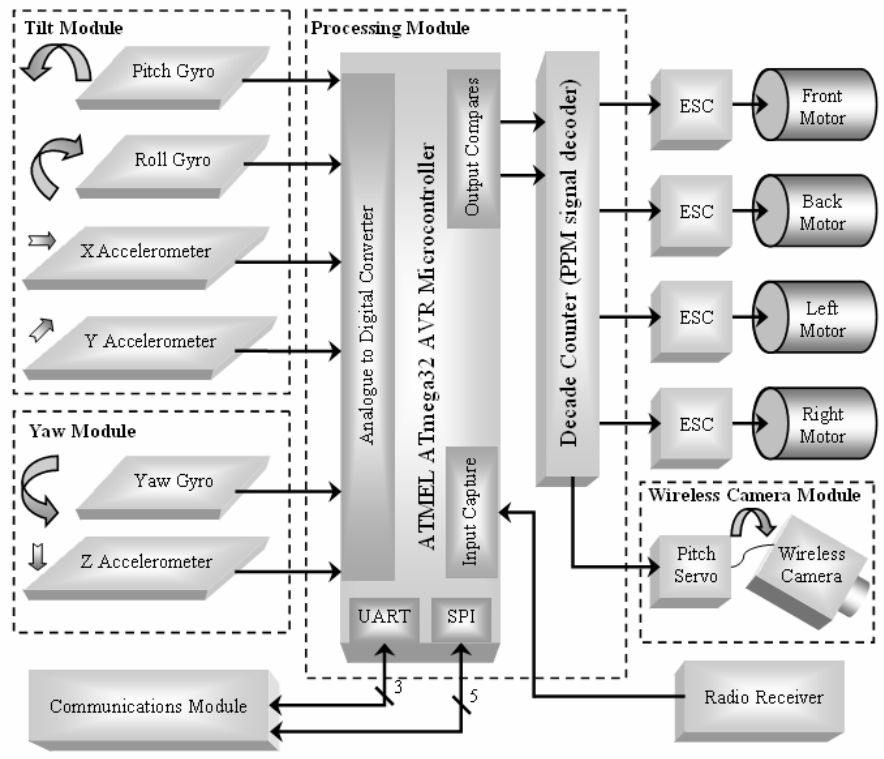

Fig. 7. QTAR Control Electronics Block Diagram

6 Control Electronics

Each system module illustrated in the block diagram of Fig. 7 either has its own removable circuit board or sub-assembly making it modular and upgradeable.

Inertial Measurement Modules

Since beginning the QTAR project, two different quadrotor aircraft have become available with attitude sensing onboard, however, they both have their limitations. The mechanical reference gyro on the Silverlit™ X-UFO is suitable for a toy, but for a UAV, it cannot operate for extended periods of time without drifting or becoming unstable. The thermal sensors on the Draganflyer™ only operate outdoors above the urban canopy in Visual Meteorological Conditions (VMC). To avoid these limitations and operate both indoors and outdoors, the QTAR system implemented low-cost inertial sensors and fused their complementary characteristics to estimate attitude using software.

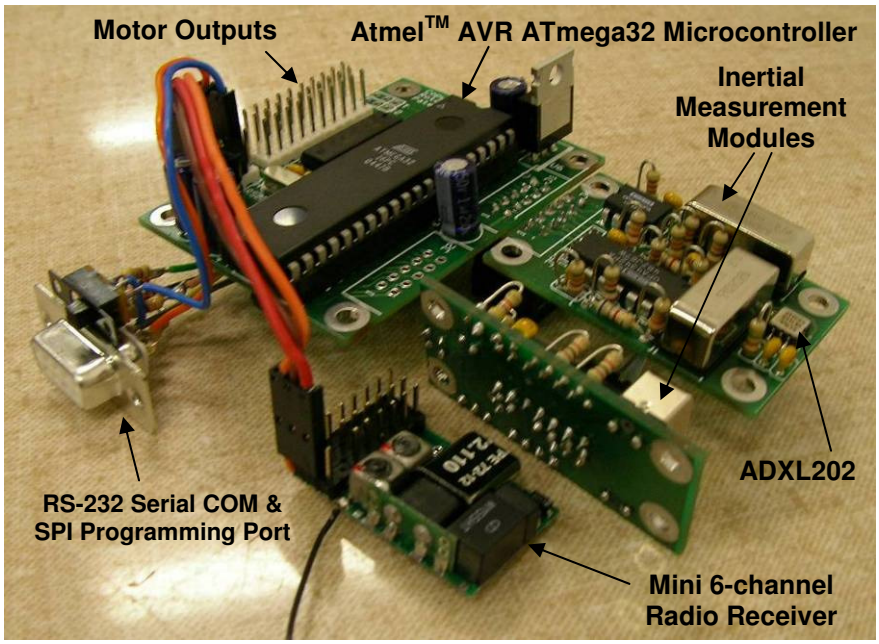

Fig. 8. Electronics Modules Laid Out Prior to Mounting

Micro Electro-Mechanical Sensor (MEMS) gyroscopes (gyros) measure angular rate/velocity around one axis. Theoretically a set of three orthogonally mounted gyros could be recursively integrated to continuously track attitude. Unfortunately, sensor bias drift and signal noise behaviour for low-cost gyros

make this unrealisable. High-performance Ring-Laser gyros are far more accurate, however, their cost and weight make them impractical for the QTAR system. The result of integrating (discretely summing) MEMS gyros is an accumulation of the bias and signal noise errors, consequently increasing the uncertainty of the attitude estimation. Without bounding this accumulated error, the estimation becomes unstable or unusable. The magnitude of this uncertainty is linearly proportional to the integration time, making these gyro sensors only good for short term estimation (ie. high frequency performance). The Tokin gyros were used in the QTAR (metal rectangular prism sensors in Fig. 8) because they were the cheapest angular rate sensors at the time.

MEMS accelerometers are implemented to compliment the gyros and bound the estimation error. Accelerometers measure both static acceleration due to gravity and dynamic acceleration due to forces on the vehicle. In steady state, a set of three orthogonally mounted accelerometers can accurately measure the pitch and roll tilt angles relative to the gravity vector. In mid flight, they also measure the collective thrust and any external disturbances like wind. Significant acceleration due to gearbox chatter and vibration introduces severe signal noise.

At the time of developing the QTAR Inertial Management Unit (IMU), the Analog Devices™ biaxial ADXL202 (±2g range) accelerometers were the best solution. Two were mounted perpendicularly to sense all three axes. The maximum angles of incline were relatively small (±15°) so a linear approximation was used to relate the horizontal accelerators to the respective tilt angles, thus avoiding complex and time-consuming trigonometric functions in firmware.

7 Attitude Estimation

As mentioned before, performing integration on the gyros to estimate tilt angle is only accurate for a short period before eventually drifting. Accelerometer data is not always a precise measurement of tilt but remains stable and bounded over an extended period of time. Therefore, a discrete recursive complementary filter was implemented in software to benefit from both sensor characteristics and estimate the tilt angle states. Since this was being performed on a microcontroller, it was developed using scaled integer arithmetic and without the aid of matrix operations in order to minimise processing time. Fig. 9 illustrates the final angular tilt state estimator, including the integer scaling factors used to maintain high accuracy without using floating point arithmetic. (Accelerometer output a = acceleration)

The result of this compensating process is a calculated angle, dominated on the short term by the gyro sensor and bounded over the long term by the accelerometer data, where K_{est} determines these time scales. Mathematically, this recursive discrete state estimator can be written as

$$\theta_{\text{est}} = \left(\theta_{\text{previous}} + \Delta\theta_{\text{gyro}}\right) + \left[\frac{\sum a}{2} - \left(\theta_{\text{previous}} + \Delta\theta_{\text{gyro}}\right)\right] K_{\text{est}} \tag{16}$$

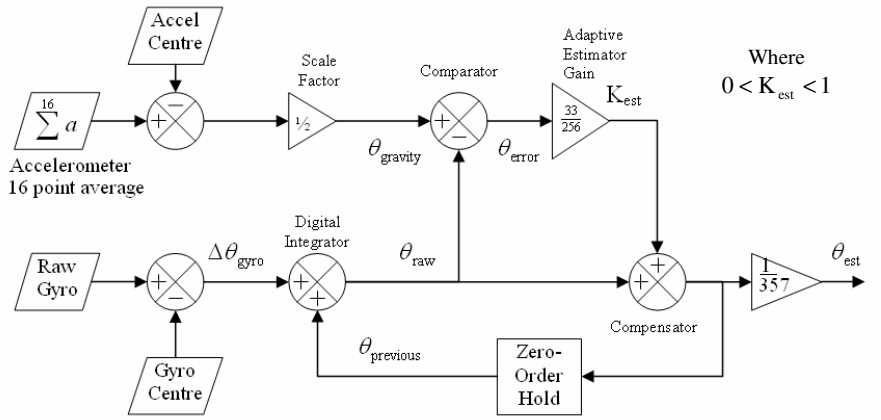

Fig. 9. Tilt Angle State Estimator

This angle estimator was simulated in MATLAB™ using inertial sensor data from flight tests. It was then implemented in firmware on the microcontroller with the scaled integer arithmetic. The experimental angle estimation data plotted in Fig. 10 demonstrates the effectiveness of the estimator in practice.

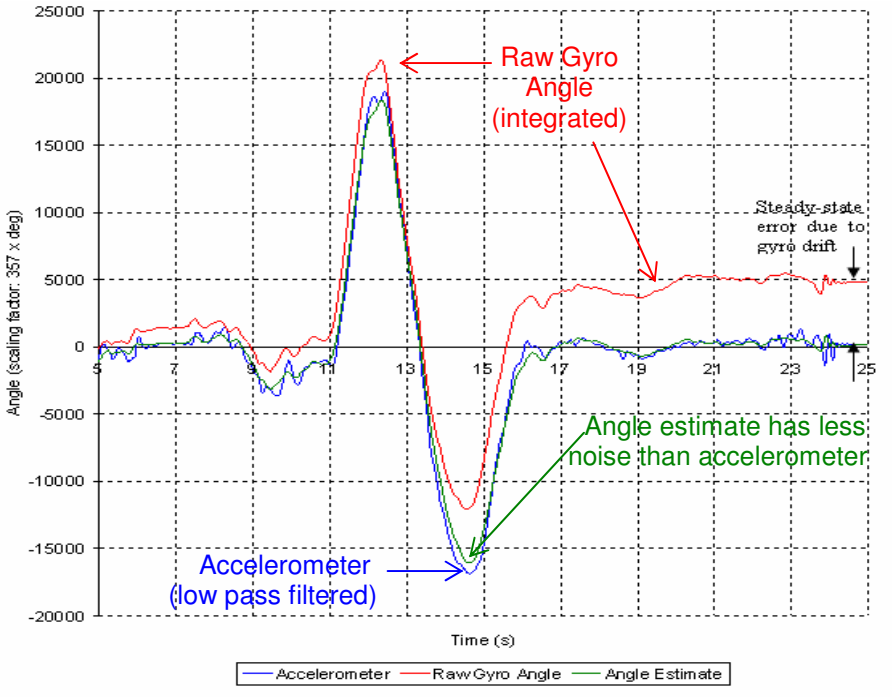

Fig. 10. Experimental Angle Estimation Data

The test was performed with the motors running to ensure the accelerometers were experiencing typical vibration noise. The plot compares the estimated angle with the uncompensated integrated gyro angle and the raw low-passed accelerometer.

It can be seen that a steady state error will occur on the gyro integration if not bounded by the accelerometers. Also, the estimator rejects most high frequency accelerometer disturbances while also responding faster than the latent low-pass filtered accelerometer.

An adaptive gain was implemented on the estimator gain K_{est} in Fig. 9. It was determined that higher rates of change in acceleration (Jerk) meant that the accelerometer was predominantly sensing dynamic acceleration. To improve the tilt angle estimation, the estimator gain was adapted to give less credibility to the accelerometer when jerk was high, but more when jerk was low.

8 Attitude Controller Implementation

The tilt angle controller gains determined from simulation were experimentally evaluated first with a 15° step input for the tilt command, but the response was underdamped. The rate gain was increased slightly and the proportional gain was lowered for improved performance. After tuning, step responses for tilt angle commands like those shown in Fig. 11 were obtained. With these tuned controller gains it was found that the system would no longer overshoot or oscillate, however, greater stability or damping comes at the cost of slower response times.

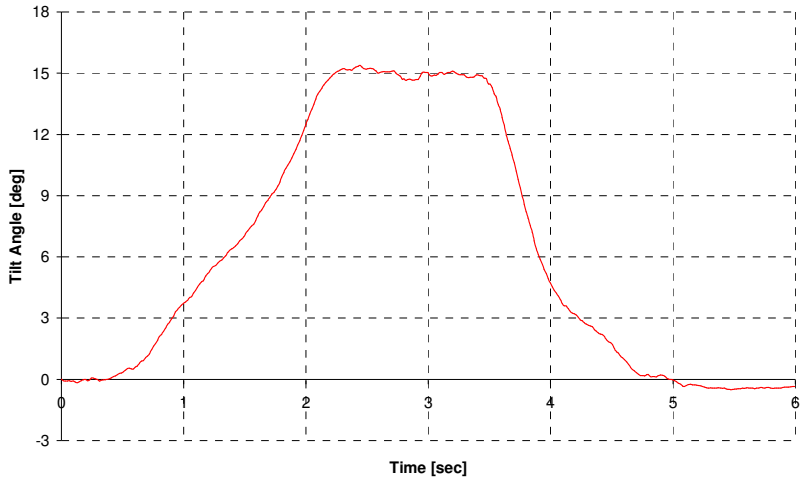

Fig. 11. Step Response with Tuned Controller Gains

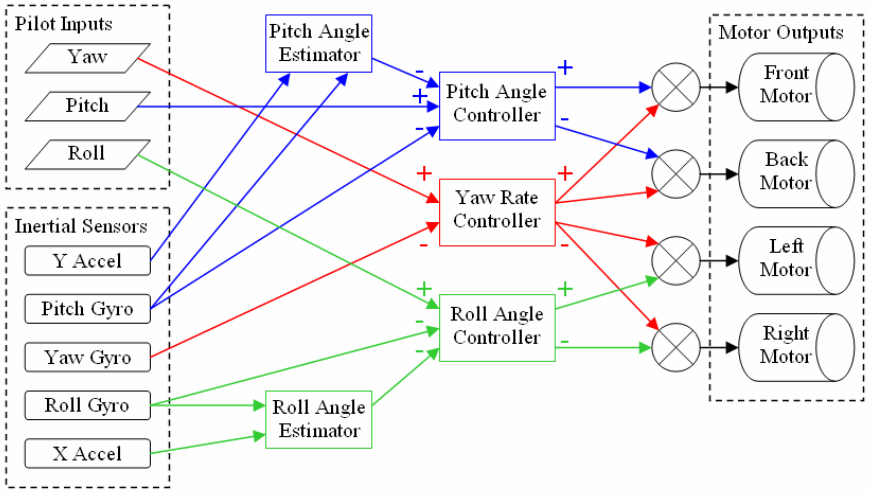

Fig. 12. Signal flow diagram for the QTAR ACS (Attitude Control System)

High level code for the QTAR ACS was written to target the Atmel™ AVR ATmega32 8-bit microcontroller using the signals shown in Fig. 12. A 4-channel (2-joystick) radio transmitter was used to send Pulse Position Modulated (PPM) signals for yaw, pitch, thrust and roll to QTAR's 6-channel radio receiver in Fig. 8.

9 Conclusions

The QTAR attitude control system successfully estimated and controlled attitude both indoors and outdoors, allowing stable hover and easily controllable omnidirectional flight as described in Fig. 3. To the best of the authors' knowledge at this time of writing, the Jerk-based adaptive tilt estimator gain method described in this paper had not been described in previous attitude estimation literature.

The final QTAR prototype was capable of carrying a 200 gram payload, while maintaining a 2:1 thrust/weight ratio and achieving flight times of around 15-20 minutes. The total cost of parts and materials for the QTAR was about AUD$870 (Australian), making it suitable for mass production and many light-weight VTOL UAV applications. The authors would like to thank Andre Turner from www.radiocontrolled.com.au [13] for sponsoring the QTAR project.

10 References

[1] Altug, E., J. P. Ostrowski, et al. (2002). Control of a quadrotor helicopter using visual feedback. Robotics and Automation, 2002. Proceedings. ICRA '02.

[2] Altug, E., J. P. Ostrowski, et al. (2003). Quadrotor control using dual camera visual feedback. Robotics and Automation, 2003. Proceedings. ICRA '03. IEEE International Conference on.

[3] Castillo, P., A. Dzul, et al. (2004). "Real-time stabilization and tracking of a four-rotor mini rotorcraft." Control Systems Technology, IEEE Transactions on **12**(4): 510-516.

[4] Coleman, C. P. (1997). A Survey of Theorectical and Experimental Coaxial Rotor Aerodynamic. California, Ames Research Center.

[5] Dienlin, D. S. and S. Dolch. (2002). "TriBelle - The Innovative Helicopter." from http://braunmod.de/etribelle.htm.

[6] Innovations, D. (2005). "RC Toys Website." http://www.rctoys.com.

[7] McKerrow, P. (2004). Modelling the Draganflyer four-rotor helicopter. Robotics and Automation, 2004. Proceedings. ICRA '04. 2004 IEEE International Conference on.

[8] Microdrones GmbH (2006). http://www.microdrones.com

[9] Petrosyan, E. (2003, 27 March 2003). "Aerodynamic Features of Coaxial Configuration Helicopter." 2006, from http://www.kamov.ru/market/news/petr11.htm.

[10] Portlock, J. (2005). QTAR: Quad Thrust Aerial Robot 2005 Video. Perth. http://www.youtube.com/watch?v=MLxe3FuQ3v0

[11] Suter, D., T. Hamel, et al. (2002). Visual servo control using homography estimation for the stabilization of an X4-flyer. Decision and Control, 2002, Proceedings of the 41st IEEE Conference on.

[12] Taylor, B., C. Bil, et al. (2003). Horizon Sensing Attitude Stabilisation: A VMC Autopilot. 18th International UAV Systems Conference, Bristol, UK.

[13] Turner, A. (2006). "Radio Controlled" website. www.radiocontrolled.com.au .

[14]